THE JOURNAL OF PHYSICAL CHEMISTRY Letters

Letter

pubs.acs.org/JPCL

Influence of Tetraalkylammonium Cation Chain Length on Gold and Glassy Carbon Electrode Interfaces for Alkali Metal−Oxygen Batteries

Iain M. Aldous and Laurence J. Hardwick*

Department of Chemistry, Stephenson Institute for Renewable Energy, University of Liverpool, Chadwick Building, Peach Street, Liverpool, Merseyside L69 7ZF, United Kingdom

Supporting Information

ABSTRACT: Fundamental studies of dioxygen electrochemistry relevant to metal−air batteries commonly require conductive supporting salts, such as tetraalkylammonium, to sustain redox processes in nonaqueous electrolytes. Electrochemical analysis of the formation and oxidation of superoxide on glassy carbon and gold working electrodes has shown a decrease in reversibility and lowering of the oxygen reduction rate constant when tetraalkylammonium cation alkyl chain length is increased. Probing interfacial regions on Au using in situ surface enhanced Raman spectroscopy (SERS) provides evidence that this is caused by the changing adsorption characteristics of tetralkylammonium cations under negative potentials. These effects are heightened with longer alkyl chain lengths, therefore reducing the reversibility of superoxide formation and dioxygen evolution. From these observations it can be established that shorter chain tetraalkylammonium cations while retaining necessary conductive support: (1) enhance reversibility and rate of superoxide formation and oxidation and (2) for in situ SERS, have lower preference for adsorption, thus improving experimental detection of superoxide at the Au electrode interface.

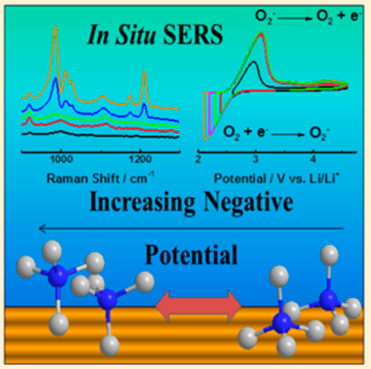

SECTION: Energy Conversion and Storage; Energy and Charge Transport

Significant attention on rechargeable alkali−metal oxygen batteries results from their high theoretical specific energies (Li−O_2 3505 Wh kg^{-1}, Na−O_2, 1581 Wh kg^{-1}, and K−O_2, 1323 Wh kg^{-1}).[1−6] The main focus of research efforts is on the development of a stable cathode and electrolyte.[1,7] To assess the viability of such systems, fundamental spectroelectrochemistry of electrode interfacial regions is required to reveal mechanistic detail of oxygen reduction and oxygen evolution reactions (ORR/OER) in nonaqueous media.[8−12] The prerequisite is the production of superoxide (one electron reduction of dioxygen), which until its direct detection by electron spin resonance in an oxygen involved enzymatic reaction was considered a reactant of minor interest.[13−16] Subsequent studies of metalloprotein catalysis (superoxide dismutase, SOD) of superoxide disproportionation (eq 1) encouraged a major renewal in superoxide chemistry[16]

$$2O_2^- + 2H^+ + SOD \leftrightarrows O_2 + H_2O_2 \quad (1)$$

The equivalent electrochemical reduction of oxygen to superoxide was explored in aqueous and nonaqueous media and found to be a quasireversible process across varying families of nonaqueous solvents (amides, ethers, nitriles, and sulfoxides).[15,17] Mechanistic dependence of oxygen reduction in the presence of alkali metals cations has recently been recognized to heavily rely on electrolyte configuration.[8−12,18−20] Increasing cation size improves the stabilization of reduced oxygen species and, hence, affects the overall electrochemical mechanism.[5,21] Larger alkali metals show similar electrochemical characteristics to tetrabutylammonium (TBA^+) salts which are commonly used as a conductive support to ascertain the stability of ORR/OER in nonaqueous electrolytes.[9,17] Although the anion within the supporting electrolyte has been reported to show no significant effect on ORR/OER,[10] the assessment of the effects of tetraalkylammonium cations (TAA^+) at the electrode interface for formation and oxidation of superoxide is yet to be established. It is reported that the size of the alkyl chain length of tetraalkylammonium (TAA^+) cations is influential in electron transfer processes of other electrochemical systems by adsorption of TAA^+, causing a modification of the electrode double-layer.[22] Most notably, under negative potential control, surface-screening can reduce electron transfer kinetics with increasing TAA^+ alkyl chain length with common electrochemical redox agents.[23,24] Deng et al.[25] showed that this effect is enhanced at potentials below −1.3 V vs SHE. Fawcett et al.[23] later deduced that conformational changes of TAA^+ alters adsorption characteristics, enhancing the inhibitory effect of longer alkyl chain length on redox processes.[22]

In this Letter, we evaluate TAA^+ cation alkyl chain lengths influence on electrode interface structure and the consequent

Received: September 2, 2014
Accepted: October 20, 2014
Published: October 20, 2014

   dx.doi.org/10.1021/jz501850u | J. Phys. Chem. Lett. 2014, 5, 3924−3930

Table 1. Cyclic Voltammetric Data and Rate Constants for Oxygen Reduction from Working Disc Electrodes in Oxygen Enriched 0.1 M TAAOTf in MeCN at 23 °C, 0.1 V s^{-1}

	working electrode					
	Au			GC		
property	(TEA)	(TPA)	(TBA)	(TEA)	(TPA)	(TBA)
I_{pc}/mA cm^{-2}	−4.33	−4.43	−3.52	−5.55	−5.31	−4.08
I_{pa}/mA cm^{-2}	2.85	2.83	1.88	4.18	4.06	3.3
Ep_c vs [Li/Li^+]/V	2.30	2.25	2.08	2.38	2.35	2.39
Ep_a vs [Li/Li^+]/V	2.75	2.88	2.99	2.48	2.62	2.75
ΔEp vs [Li/Li^+]/V	0.36	0.63	0.91	0.1	0.27	0.36
charge ratio (Q_a/Q_c)	0.90	0.84	0.80	0.88	0.86	0.78
peak current ratio (I_{pa}/I_{pc})/(mA)	0.73	0.63	0.53	0.61	0.73	0.83
rate constant (k^o)/cm s^{-1}	2.51×10^{-4}	1.88×10^{-4}	9.34×10^{-5}	9.14×10^{-4}	3.20×10^{-4}	2.46×10^{-4}

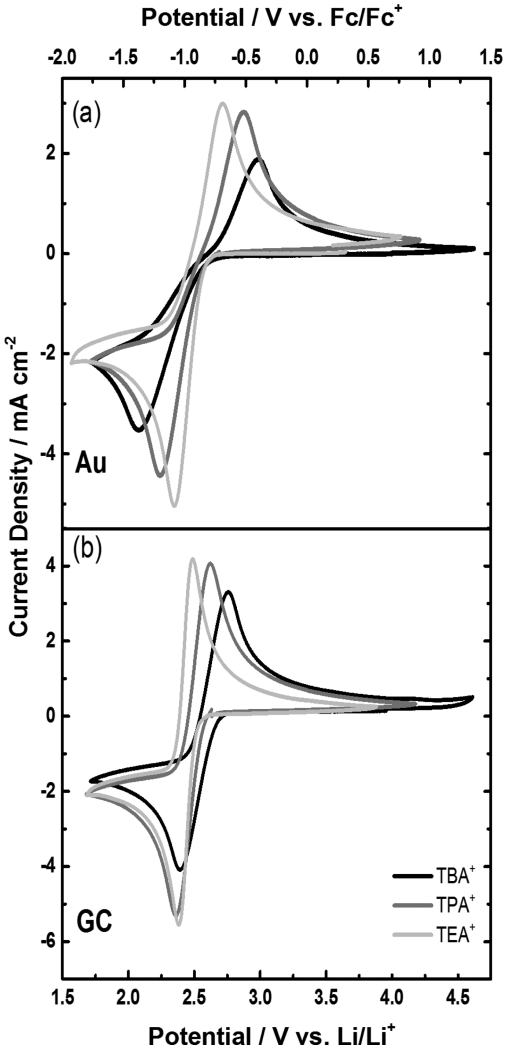

Figure 1. Superoxide formation and oxidation in oxygen enriched 0.1 M TAAOTf in MeCN with (a) Au and (b) GC working disc electrodes at 23 °C, 0.1 V s^{-1}.

effects on superoxide formation and oxidation (eq 2) via combination of electrochemical analysis and in situ surface enhanced Raman spectroscopy (SERS)

$$O_2 + e^- \leftrightarrows O_2^- \qquad E_o = 2.5 \text{ V vs Li/Li}^+ \tag{2}$$

Cyclic voltammetric (CV) studies of the formation and oxidation of superoxide chemistry were conducted in oxygen enriched 0.1 M tetraethylammonium trifluoromethanesulfonate (TEAOTf), tetrapropylammonium trifluoromethanesulfonate (TPAOTf), and tetrabutylammonium trifluoromethanesulfonate (TBAOTf) in MeCN and compared and contrasted on polycrystalline Au and glassy carbon (GC) planar working disc electrodes (Figure 1), the comparison of which show that on both Au and GC, increasing the alkyl chain length of the supporting electrolyte cation, corresponds to an increased hysteresis of oxygen redox processes and decrease in current density in agreement with previous studies.[22,26] The difference in observed peak current density and hysteresis cannot be entirely explained by the varying bulk ionic conductivities of the different electrolytes, as they are fairly similar (TEAOTf 10.8 mS cm^{-1}, TPAOTf 10.3 mS cm^{-1}, TBAOTf 9.2 mS cm^{-1}). The electrochemistry on Au shows shorter chain TAA^+ (TEA^+ and TPA^+) supported oxygen reduction and evolution is more reversible compared to when supported by longer chain analogues (TBA^+). Numerical analysis (Table 1) shows that TEA^+ and TPA^+ supported oxygen reduction and evolution display greater Coulombic efficiency and decreased hysteresis over TBA^+. Interestingly, the CV scans for GC show that on reduction the cathodic peak position is essentially unchanged by the increase in alkyl chain length. Conversely, for the oxidation of superoxide on GC, the identical trend is observed as for Au, for every increase in the chain length the anodic peak shifts positive by ca. 130 mV (Table 1).

These differences in the formation of superoxide may be explained by combining the negligible influence of formal adsorption on GC and the observation that TEA^+ and TPA^+ show similar adsorption characteristics on precious metal surfaces.[22] The implication of which is that for surfaces where adsorption is prevalent, increasing the bulkiness of TAA^+, and therefore aliphatic character of the electrode double-layer decreases the electrokinetics of superoxide formation and oxidation. The initial current rise for TBA^+ is higher in potential than other TAA^+ that may be due to the formation of a $TBAO_2$ complex, which is very similar to that seen upon the addition of small quantities of Li^+, which complexes with O_2^- to form lithium superoxide (Supporting Information Figure S1). The increased Au reduction hysteresis with longer chained TAA^+ could be explained by the greater adsorption of TAA^+ and therefore presence at the surface. In the case of TBA^+, a film is observed to form on the Au electrode surface and is identified as $TBAO_2$ (Supporting Information Figure S2a). This film may be responsible for the partial blocking of the surface and limiting the rate of oxygen reduction. On reduction, it can be seen that on GC, where precipitation of $TBAO_2$ on the electrode surface may not be as prevalent due to lower

dx.doi.org/10.1021/jz501850u | J. Phys. Chem. Lett. 2014, 5, 3924−3930

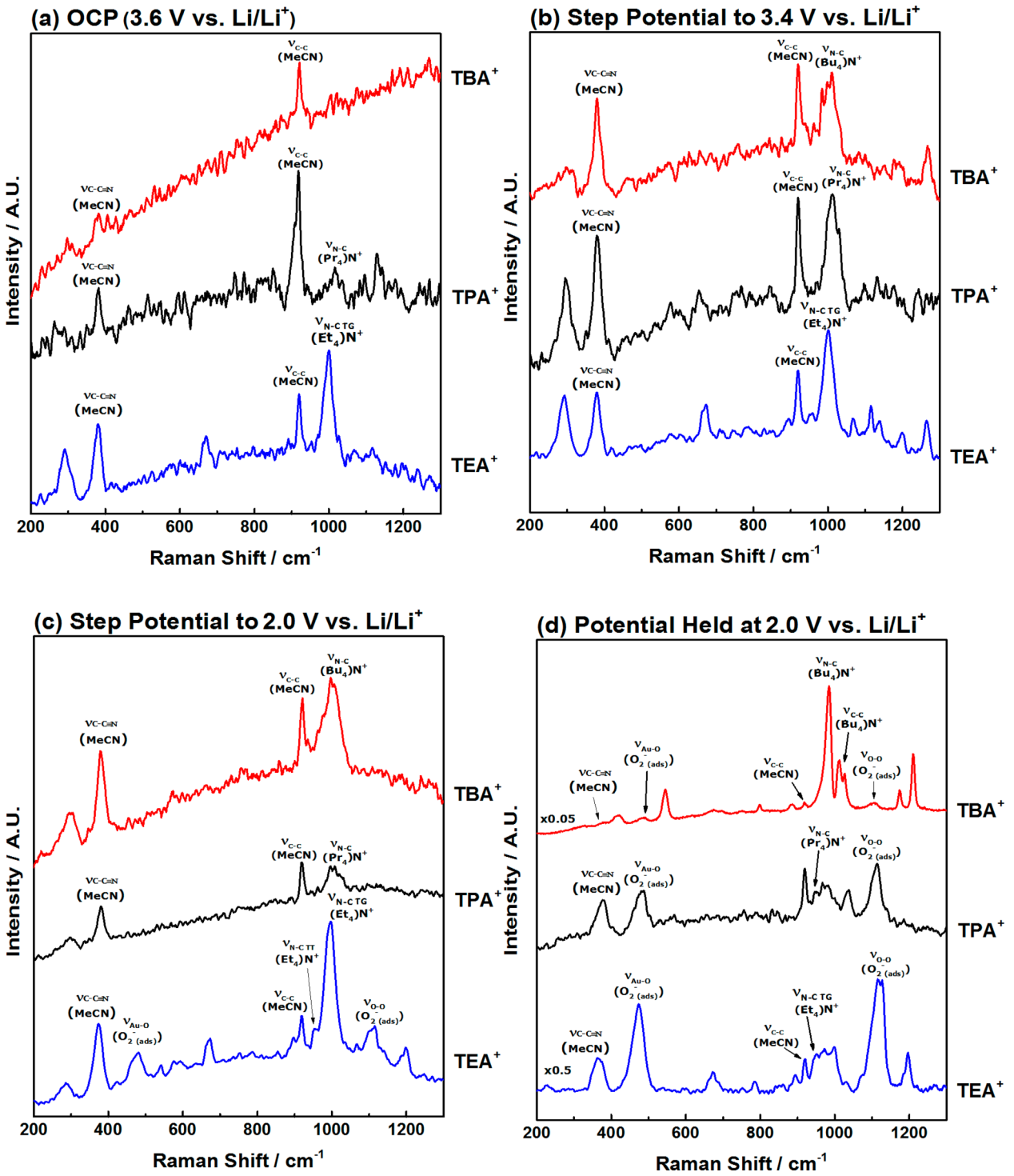

Figure 2. In situ SERS of oxygen enriched 0.1 M TAAOTf in MeCN with roughened Au working disc electrodes at 23 °C, 0.1 V s^{-1} at (a) OCP (3.6 V vs Li/Li^+), (b) 3.4 V, (c) 2.0 V, (d) holding potential at 2.0 V. Spectra are shifted arbitrarily along the *y* axis for clarity.

adsorption (Supporting Information Figure S2b), the reduction wave on the CV for all three TAA^+ are fairly similar, indicating that oxygen reduction is not hindered. However, the increased bulkiness of longer-chained $TAAO_2$ complexes in solution could explain why on both GC and Au electrodes a similar trend in the shift of oxidation peak position is observed. Rotating disk electrode experiments (RDE) reveal that in fact a decrease in electrokinetics upon the increase in TAA^+ alkyl chain length is observed on both Au and GC (Table 1 and Supporting Information Table S1 and Figures S3 and S4). The oxygen reduction rate constant (k_o) is measured to decrease by a factor of ca. 3 on both Au and GC moving from TEA^+ to TBA^+ based electrolytes (Table 1).

In situ SERS on roughened Au provides confirmation that these small changes in electrochemical response show a marked effect on the cathodic interface. OCP (3.6 V vs Li/Li^+, Figure 2a) spectra confirm that the presence of TAA^+ at the surface is initially lower before electrochemistry is performed. The

dx.doi.org/10.1021/jz501850u | J. Phys. Chem. Lett. 2014, 5, 3924−3930

Table 2. Peak Assignment and Position from in Situ SERS in Oxygen Enriched 0.1 M TAAOTf in MeCN at 23 °C, 0.1 V s^{-1} at 2.0 V vs Li/Li^+

	peak position (cm^{-1})		
peak	TEA^+	TPA^+	TBA^+
(1) ν_{c-s} (OTf^-)	288		
(2) $\nu_{C-C\equiv N}$ (MeCN)	374	376	419
(3) $\nu_{Au-O_2^-}$ ($O_2^-{}_{(ads)}$)	480	483	487
(4) $\delta_{s\ SO_3}$ (OTf^-)	673		674
(5) ν_{C-C} (MeCN)	920	919	918
(6) $\nu_{N-C\ TT}(TAA)N^+$	956	951	984
(7) $\nu_{N-C\ TG}(TAA)N^+$	997	967	1012
(8) ν_{C-C} $(TAA)N^+$		980	1026
(9) ν_{C-C} $(TAA)N^+$			1037
(10) ν_{o-o} ($O_2^-{}_{(ads)}$))	1115	1113	1105
(11) ν_{S-CF_3} (OTf^-)	1197	1183	1173
(12) ν_{C-N} (CN^-)	2108	2116	
(13) ν_{C-N} (CN^-)	2173	2182	
(14) ν_{C-N} (MeCN)	2250	2251	2250
(15) $\nu_{s(C-H)}$ (MeCN)	2941	2937	2940
(16) $\nu_{AS(C-H)}$ (MeCN)		2988	2994

highest SERS spectral intensity is observed when using shorter chain TAA^+ (TEA^+). The main features in these spectra correspond to Raman bands for MeCN (375 and 920 cm^{-1}), TEA^+ (1000 cm^{-1}), and OTf^- (288 and 673 cm^{-1}) (Table 2). Initial cycling of dioxygen redox reactions increases the TAA^+ signal as cation adsorption occurs at the interface (Figure 2b). Similar techniques have shown the effect of increasing pressure of TEA^+ in a diamond anvil cell on the Raman signal of TEA^+ confirms this peak (992 cm^{-1}) to be due to the *trans–trans trans–trans* (*tt.tt*) conformation of TAA^+.[27] This conformer is typical of TAA^+ adsorption in a tripod state, with one alkyl chain protruding into the double-layer. The signal in this region for longer-chain TPA^+ and TBA^+ is broadened and dulled comparatively in intensity compared to solvent signal for TEA^+ and the relative position increased in wavenumber displaying a lower energy C–N stretch (TEA^+ 992 cm^{-1}, TPA^+ 1012 cm^{-1}, TBA^+ 1013 cm^{-1}). However, this is believed to be due to an equivalent conformer for longer-chain TAA^+.

Although the adsorption of TAA^+ is widely accepted in this case, it is complicated by competing adsorption of both MeCN and adsorbed superoxide as shown by the differences in the ratio of the species present at the surface as you increase alkyl chain length. This is in line with the fact that at a given potential the presence of solvent molecules and thus oxygen is significantly increased when smaller ions such as TEA^+ and TPA^+ define the position of the outer Helmholtz plane.[23] This is shown in Table 3, whereby the peak intensity ratio of superoxide bands (ν_{O-O} and ν_{Au-O} ca. 1100 and 480 cm^{-1}) has been normalized vs the intensity of ν_{C-C} MeCN (ca. 920 cm^{-1}) when the potential is held at 2.0 V vs Li/Li^+ as a qualitative comparison of superoxide presence at the surface (the measured spectra did not change after a period of up to 30 min; Supporting Information Figure S5). This normalized superoxide band peak intensity shows a decreasing trend as you increase the alkyl chain length of TAA^+. This suggests that the relative presence of superoxide has decreased with longer-chain TAA^+ and supports complexation of TBA^+ and O_2^-, as seen previously in the CV data (Figure 1). Presence of superoxide at the interface appears to be greater with respect to MeCN for TEA^+ and TPA^+ than TBA^+, signifying the greater propensity of TBA^+ to adsorb to the surface. This is clearly shown by the dominance of superoxide signals in the TEA^+ spectra (Figure 2d), which is overtaken by the dominance of TAA^+ signals as you increase the alkyl chain length to TBA^+.

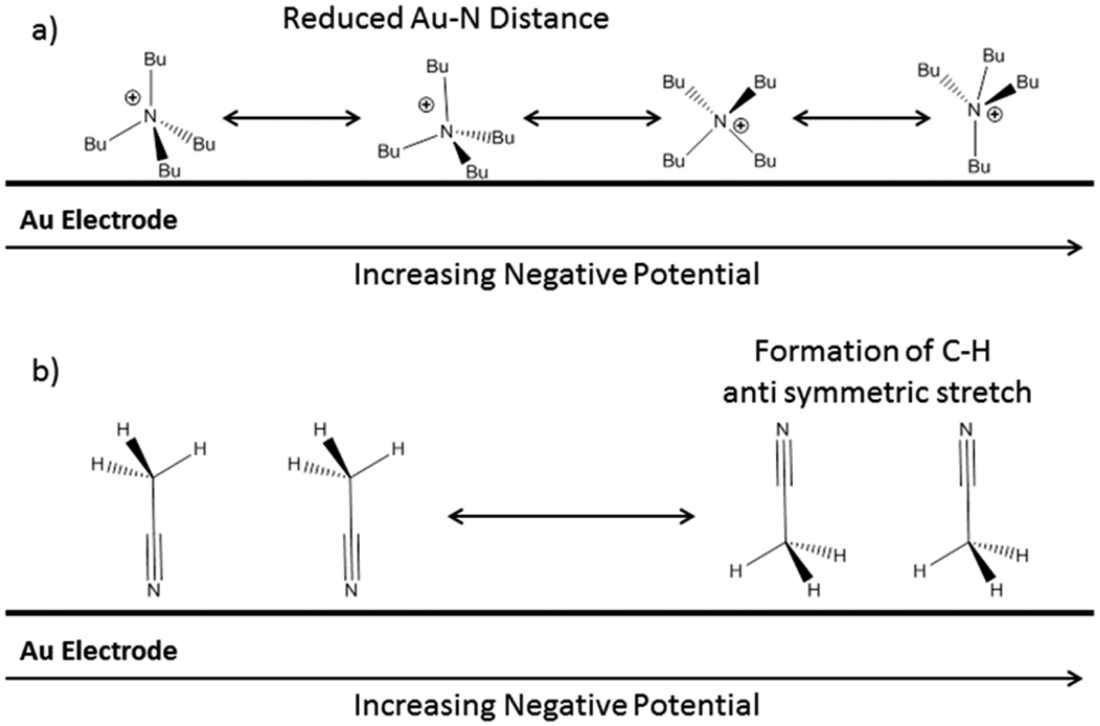

Figure 3. (a) Conformational shift of TBA^+ with increasing negative potential occurring at 2.25 V vs Li/Li^+, (b) potential dependent orientation of adsorbed MeCN on Au working electrode.

dx.doi.org/10.1021/jz501850u | J. Phys. Chem. Lett. 2014, 5, 3924–3930

Table 3. Band Position of Superoxide at 2.0 V vs Li/Li^+ in Various TAA^+ Containing Electrolytes and Peak Intensity Ratio of Superoxide Bands[a] Normalised vs Intensity of ν_{C-C} MeCN[b]

	wavenumber cm^{-1} (fwhm cm^{-1})			ratio of superoxide/acetonitrile peak intensity (ν (O_2^-)/ν_{C-C} (MeCN))		
TAA^+	TEA^+	TPA^+	TBA^+	TEA^+	TPA^+	TBA^+
ν_{O-O} (O_2^-)	1115 (39)	1113 (38)	1104 (29)	3.47	1.65	1.35
ν_{Au-O} (O_2^-)	478 (34)	480 (36)	484 (29)	4.71	1.06	1.03

[a] ν_{O-O} and ν_{Au-O}. [b] Ca. 920 cm^{-1}.

The relative exclusion of superoxide at the surface is shown in Figure 2d at 2.0 V vs Li/Li^+, as well as by the clear presence of adsorbed O_2^- with TEA^+, which is explained by the change in adsorption characteristics with longer chained TAA^+. In the specific case of TBA^+, the "*tt.tt*" conformer under negative potentials first distorts the three surface alkyl chains, thus decreasing the Au^--N^+ distance, which increases the effective screening of the electrode surface.[23] Shorter chain TEA^+ shows much more of an enhancement of the *tt.tt* conformer signal, as well as a secondary shoulder peak (956 cm^{-1}) (Figure 2c) corresponding to the formation of the *trans–gauche trans–gauche* (*tg.tg*) conformer that decreases the Au^--N^+ distance under these potential conditions.[23]

The conformation of the longer-chain TAA^+ is probed only by holding the potential at specific values (Figure 2d). By holding the potential beyond 2.25 V vs Li/Li^+, the longer-chain TBA^+ broad signal splits into three notable peaks (Supporting Information Figure S6, 1012, 1026, and 1037 cm^{-1}). The peak at 1012 cm^{-1} is the "*tt.tt*" conformation of TBA^+ but is more intense due the distorted and therefore restricted alkyl chains. The two other peaks can be assigned as ν_{c-c} $(Bu)_4N^+$ from conformational changes occurring beyond the potential of zero charge (pzc). Deng et al.[25] proposed that under reducing potentials, the adsorption of TBA^+ and longer alkyl chains coincides with those shown in Figure 3a.[25] Negative of the pzc, which is believed to be at 2.25 V vs Li/Li^+ in this case due to the band splitting (Supporting Information Figure S6), the *tt.tt* conformer and its distorted configurations are the general state of adsorbed TAA^+ on the surface. At the pzc, there is a loss of one alkyl chain at the surface, and beyond this, the loss of a second alkyl chain leaving only one bound (Figure 3a). The constraints on the alkyl chains are therefore removed and therefore the skeletal alkyl chain vibrations can be observed. Consequently, beyond the pzc of TBA^+, it is increasingly difficult to reduce oxygen at the surface due to the increased aliphatic character and, therefore, steric hindrance of the double-layer. This may lower electrokinetics across the layer further, which may explain why a second electron reduction peak is difficult to ascertain and characterize at these potentials utilizing TBA^+ as a supporting salt for oxygen redox processes.[25,28]

The effect that the different cations have on dioxygen electrochemistry at the surface is observed from the peak position of TAA^+ coordinated superoxide (Tables 2 and 3). TAA^+ coordinated superoxide's wavenumber decreases with increasing chain length, which shows that the O–O bond is weaker and therefore has greater radical character, the consequence of which is that shorter chain TAA^+ moderate the radical character of TAA^+ coordinated superoxide in solution. Furthermore, the band position of the $Au-O_2^-{}_{(ads)}$ is seen to increase with larger TAA^+ showing that the increased radical character of superoxide results in a marginally stronger interaction with the Au surface. Therefore, shorter chain TAA^+ permits both improved oxygen redox kinetics and formation of a less reactive superoxide species.

These findings are relevant to practical batteries, considering the fact that Read et al.[26] reported the addition of TBA^+ to an electrolyte enhances the discharge capacity of a $Li-O_2$ cell. They based the increase of capacity on the fact that the quaternary ammonium salts acts as a pseudophase transfer catalyst (pptc). In organic chemistry, it is commonly found although TBA^+ salts are efficient catalysts that many processes favor smaller, hydrophilic TAA^+. Therefore, considering the changes in superoxide reactivity in solution, care should be taken when choosing the chain length of pptc for $Li-O_2$ batteries.[29] The preferential catalytic activity sometimes observed for shorter chain TAA^+ salts is explained by Solaro et al.[29] by the accessibility of the charged nitrogen center being able to more effectively bind the substrate anion more than those shielded by longer alkyl chains.[26] In this situation, this would mean that the adsorbed TAA^+ "monolayer" acts as mediator between adsorbed superoxide and its transfer to solution. Whether this process facilitates the removal of Li_xO_y into solution, when Li^+ are present, or only the removal of superoxide, is still under investigation; however, we believe that the use of pptc's would be a useful future strategy in the prevention of formation of dense insulating metal oxide layers on porous electrode surfaces.[28]

The preferential solvation of superoxide by TBA^+ over smaller cations (Li^+) is in line with present explanation of the electrochemical mechanism of $metal-O_2$ using hard soft acid base theory (HSAB), whereby smaller cations are harder Lewis acids and thus cannot stabilize softer bases such as superoxide as well as larger softer cations.[9] Therefore, TBA^+ will support the solvation and transfer of superoxide from the surface more than shorter chain TAA^+, which is suggested by the SERS data within Figure 2c, where the superoxide generated within TBA^+ has left the electrode and hence not detectable. The surface screening effect of TBA^+ then justifies the findings that above a certain concentration of TBA^+ added to an electrolyte, the discharge capacity decreases as adsorption processes diminish the reversibility of superoxide formation/oxidation.[26]

Solvent orientation within the electrode double-layer is also dependent on potential and from this method it is possible to describe this orientation by analyzing the C–H stretches of MeCN (Figure 4a).[30] Here, it can be seen that as increasingly reductive potentials are applied, the antisymmetric C–H stretch of MeCN forms a shoulder peak in the spectra. This displays a shift of solvent orientation as shown from adsorption via the CN to adsorption via the methyl group (Figure 3b). The reason for the appearance of the antisymmetric stretch is due to the restricted rotation of methyl hydrogen atoms when adsorbed on the surface.[30] Analogous to this and to further substantiate the increased presence of solvent molecules at the surface the lack of CN^- bands at 2115 and 2180 cm^{-1} (Figure 4b) when using longer-chain TBA^+ shows a decrease in the

dx.doi.org/10.1021/jz501850u | J. Phys. Chem. Lett. 2014, 5, 3924–3930

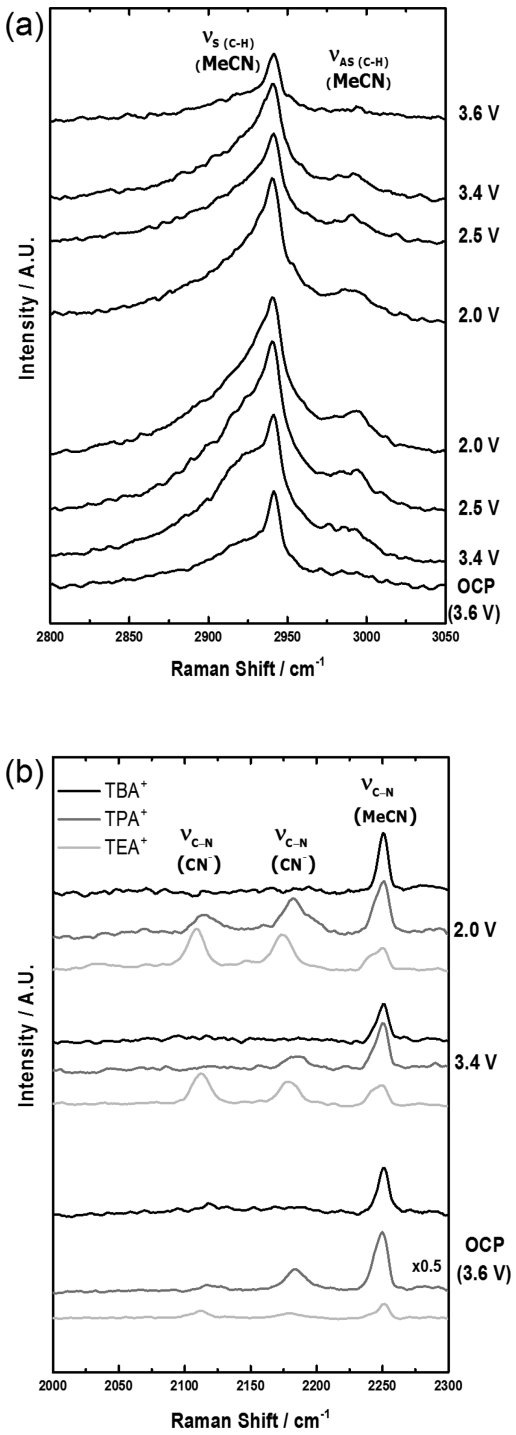

Figure 4. (a) In situ SERS showing influence of potential on CN^- stretching region in oxygen enriched 0.1 M TEAOTf in MeCN and (b) C−H stretching region of MeCN cycled within various TAA^+ supporting salts, with roughened Au working disc electrodes at 23 °C, 0.1 V s^{-1}.

amount of available roughened Au catalytic sites on which solvent decomposition can occur.[31] This is due to adsorption of longer alkyl chain TAA^+ at high reduction potentials displacing solvent molecules and, therefore, reducing the amount of catalytic sites on the roughened gold surface. Indicatively, this will also decrease the amount of superoxide adsorbed at the surface that leads us to suggest electron transfer occurs through an outer sphere mechanism, heavily reliant on the probability of electron tunnelling occurring with TBA^+ supported oxygen redox processes.

The assessment of tetraalkylammonium cations has demonstrated that length of the alkyl chain can significantly alter the Au electrode interface and enhance or hinder aspects of oxygen redox kinetics. The effects of conformational changes of different alkyl chain lengths at high reduction potentials has been characterized using in situ surface enhanced Raman spectroscopy enabling the deduction of the effects this has on oxygen redox processes. Longer-chain TAA^+ show an increased hysteresis and greater irreversibility over shorter chain TAA^+, as a result of the conformational changes of adsorbed TAA^+ under increasingly negative potentials. These changes result from the increasing aliphatic character of the double-layer. This slows the rate of electrokinetics at both the Au and GC electrode interfaces, as shown by RDE experiments (Table 1, Supporting Information Figures S3 S4), thereby resulting in lowering the probability of electron transfer and causing the measured progressive electrochemical hysteresis within cyclic voltammograms. Caution should be taken during kinetic studies of electrocatalysts utilizing supporting salts, as they play a significant role in determining reaction rates of dioxygen in nonaqueous solvents. However, although the presence of superoxide and acetonitrile is decreased at the surface when using longer-chain TAA^+ supported oxygen reduction, the presence of TBA^+ inherently protects the surface from catalytic side reactions due to the SERS enhancement produced by the Au roughening procedure. Nevertheless, the use of shorter chain TAA^+ are recommended as supporting salts in SERS studies because of the greater sensitivity to detect reduced oxygen species due to lower competitive absorption from supporting salt.

■ ASSOCIATED CONTENT

Ⓢ Supporting Information

Methods section and synthesis of tetrapropylammonium trifluoromethanesulfonate, supporting cyclic voltammetry, rotating disk electrode data and SERS and ex situ Raman spectra. This material is available free of charge via the Internet http://pubs.acs.org.

■ AUTHOR INFORMATION

Corresponding Author

*E-mail: hardwick@liverpool.ac.uk.

Notes

The authors declare no competing financial interest.

■ ACKNOWLEDGMENTS

The authors would like to gratefully acknowledge discussions with Prof. Richard Nichols and financial support from the Engineering and Physical Sciences Research Council (EPSRC), U.K., under grant number EP/J020265/1.

■ REFERENCES

(1) Bruce, P. G.; Freunberger, S. A.; Hardwick, L. J.; Tarascon, J.-M. Li−O_2 and Li−S Batteries with High Energy Storage. *Nat. Mater.* **2012**, *11*, 19−29.

(2) Christensen, J.; Albertus, P.; Sanchez-Carrera, R. S.; Lohmann, T.; Kozinsky, B.; Liedtke, R.; Ahmed, J.; Kojic, A. A Critical Review of Li/Air Batteries. *J. Electrochem. Soc.* **2011**, *159*, R1−R30.

(3) Das, S. K.; Lau, S.; Archer, L. A. Sodium−Oxygen Batteries: A New Class of Metal-Air Batteries. *J. Mater. Chem. A* **2014**, *2*, 12623−12629.

(4) Ren, X.; Wu, Y. A Low-Overpotential Potassium−Oxygen Battery Based on Potassium Superoxide. *J. Am. Chem. Soc.* **2013**, *135*, 2923−2926.
(5) Hartmann, P.; Bender, C. L.; Vračar, M.; Dürr, A. K.; Garsuch, A.; Janek, J.; Adelhelm, P. A Rechargeable Room-Temperature Sodium Superoxide (NaO_2) Battery. *Nat. Mater.* **2013**, *12*, 228−232.
(6) Girishkumar, G.; McCloskey, B.; Luntz, A. C.; Swanson, S.; Wilcke, W. Lithium−Air Battery: Promise and Challenges. *J. Phys. Chem. Lett.* **2010**, *1*, 2193−2203.
(7) Hardwick, L. J.; Bruce, P. G. The Pursuit of Rechargeable Non-Aqueous Lithium−Oxygen Battery Cathodes. *Curr. Opin. Solid State Mater. Sci.* **2012**, *16*, 178−185.
(8) Peng, Z.; Freunberger, S. A.; Hardwick, L. J.; Chen, Y.; Giordani, V.; Bardé, F.; Novák, P.; Graham, D.; Tarascon, J.-M.; Bruce, P. G. Oxygen Reactions in a Non-Aqueous Li^+ Electrolyte. *Angew. Chem., Int. Ed.* **2011**, *50*, 6351−6355.
(9) Laoire, C. O.; Mukerjee, S.; Abraham, K. M.; Plichta, E. J.; Hendrickson, M. A. Elucidating the Mechanism of Oxygen Reduction for Lithium-Air Battery Applications. *J. Phys. Chem. C* **2009**, *113*, 20127−20134.
(10) Freunberger, S. A.; Chen, Y.; Drewett, N. E.; Hardwick, L. J.; Bardé, F.; Bruce, P. G. The Lithium−Oxygen Battery with Ether-Based Electrolytes. *Angew. Chem., Int. Ed.* **2011**, *50*, 8609−8613.
(11) Mizuno, F.; Nakanishi, S.; Kotani, Y.; Yokoishi, S.; Iba, H. Rechargeable Li−Air Batteries with Carbonate-Based Liquid Electrolytes. *Electrochemistry* **2010**, *78*, 403−405.
(12) Bryantsev, V. S.; Uddin, J.; Giordani, V.; Walker, W.; Addison, D.; Chase, G. V. The Identification of Stable Solvents for Nonaqueous Rechargeable Li-Air Batteries. *J. Electrochem. Soc.* **2013**, *160*, A160−A171.
(13) Chin, D. H.; Chiericato, G.; Nanni, E. J.; Sawyer, D. T. Proton-Induced Disproportionation of Superoxide Ion in Aprotic Media. *Anal. Chem.* **1982**, *104*, 1296−1299.
(14) Knowles, P. F.; Gibson, J. F.; Pick, F. M.; Bray, R. C. Electron-Spin-Resonance Evidence for Enzymic Reduction of Oxygen to a Free Radical, the Superoxide Ion. *J. Biochem.* **1969**, *111*, 53−58.
(15) Sawyer, D. T.; Calderwood, T. S.; Yamaguchi, K.; Angelis, C. T. Synthesis and Characterization of Tetramethylammonium Superoxide. *Inorg. Chem.* **1983**, *22*, 2577−2583.
(16) Sawyer, D. T.; Valentine, J. S. How Super is Superoxide? *Acc. Chem. Res.* **1981**, *14*, 393−400.
(17) Sawyer, D. T.; Roberts, J. L., Jr. Electrochemistry of Oxygen and Superoxide Ion in Dimethylsulfoxide at Platinum, Gold and Mercury electrodes. *J. Electroanal. Chem.* **1966**, *12*, 90−101.
(18) Mizuno, F.; N, S.; Kotani, Y.; Yokoishi, S.; Iba, H. Enhancing Effect of Carbon Surface in the Non-Aqueous Li-O_2 Battery Cathode. *Electrochemistry* **2010**, *78*, 403−405.
(19) Lodge, A. W.; Lacey, M. J.; Fitt, M.; Garcia-Araez, N.; Owen, J. R. Critical Appraisal on the Role of Catalysts for the Oxygen Reduction Reaction in Lithium-Oxygen Batteries. *Electrochim. Acta* **2014**, *140*, 168−173.
(20) Mozhzhukhina, N.; Méndez De Leo, L. P.; Calvo, E. J. Infrared Spectroscopy Studies on Stability of Dimethyl Sulfoxide for Application in a Li−Air Battery. *J. Phys. Chem. C* **2013**, *117*, 18375−18380.
(21) Laoire, C. O.; Mukerjee, S.; Abraham, K. M.; Plichta, E. J.; Hendrickson, M. A. Influence of Nonaqueous Solvents on the Electrochemistry of Oxygen in the Rechargeable Lithium−Air Battery. *J. Phys. Chem. C* **2010**, *114*, 9178−9186.
(22) Gennaro, A.; Isse, A. A.; Giussani, E.; Mussini, P. R.; Primerano, I.; Rossi, M. Relationship Between Supporting Electrolyte Bulkiness and Dissociative Electron Transfer at Catalytic and Non-Catalytic Electrodes. *Electrochim. Acta* **2013**, *89*, 52−62.
(23) Fawcett, W. R.; Fedurco, M.; Opallo, M. The Inhibiting Effects of Tetraalkylammonium Cations on Simple Heterogeneous Electron Transfer Reactions in Polar Aprotic Solvents. *J. Phys. Chem.* **1992**, *96*, 9959−9964.
(24) Petersen, R. A.; Evans, D. H. Heterogeneous Electron Transfer Kinetics for a Variety of Organic Electrode Reactions at the Mercury−Acetonitrile Interface Using Either Tetraethylammonium Perchlorate or Tetraheptylammonium Perchlorate Electrolyte. *J. Electroanal. Chem.* **1987**, *222*, 129−150.
(25) Deng, Z.; Irish, D. E. Potential Dependence of the Orientation of $(CH_3)_4N^+$ Adsorbed on a Silver Electrode. A SERS Investigation. *J. Phys. Chem.* **1994**, *98*, 9371−9373.
(26) Zhang, S. S.; Foster, D.; Read, J. The Effect of Quaternary Ammonium on Discharge Characteristic of a Non-Aqueous Electrolyte Li/O_2 Battery. *Electrochim. Acta* **2011**, *56*, 1283−1287.
(27) Takekiyo, T.; Yoshimura, Y. Raman Spectroscopic Study on the Hydration Structures of Tetraethylammonium Cation in Water. *J. Phys. Chem. A* **2006**, *110*, 10829−10833.
(28) Mason, D.; Magdassi, S.; Sasson, Y. Interfacial Activity of Quaternary Salts as a Guide to Catalytic Performance in Phase-Transfer Catalysis. *J. Org. Chem.* **1990**, *55*, 2714−2717.
(29) Solaro, R.; D'Antone, S.; Chiellini, E. Heterogeneous Ethylation of Phenylacetonitrile. *J. Org. Chem.* **1980**, *45*, 4179−4183.
(30) Baldelli, S.; Mailhot, G.; Ross, P.; Shen, Y. R.; Somorjai, G. A. Potential Dependent Orientation of Acetonitrile on Platinum (111) Electrode Surface Studied by Sum Frequency Generation. *J. Phys. Chem. B* **2001**, *105*, 654−662.
(31) Cao, P.; Sun, Y. On the Occurrence of Competitive Adsorption at the Platinum−Acetonitrile Interface by Using Surface-Enhanced Raman Spectroscopy. *J. Phys. Chem. B* **2003**, *107*, 5818−5824.